

# Gaining Intuition for Diving Birds: Wedges and Cones as a Model for Beak-Water Impact

TALIA WEISS, Virginia Tech

---

Gannets (*Morus spp.*) have the remarkable ability to dive into the water from up to 30 m high - hitting the water's surface at 24 m/s. It has been assumed in the past that when impacting the water these birds encounter a large force due to the massive density change from air to water. Despite this, these birds are rarely injured during a dive, and will dive up to 100 times in a single trip. While both intuition and complex CFD models have predicted that gannets will experience a massive deceleration upon water impact, experimental studies have yet to measure large acceleration changes on live diving birds in the field. In order to gain insight into the amount of acceleration these birds may feel during a dive, and over what timescales such accelerations occur, it is useful to model the plunge dive as simply as possible. The goal of this paper was to model the bird's beak (and body) as either a 2D wedge or a cone, and using cone/wedge angles measured from real bird skeletons as well as mass and velocity estimates from literature, compare accelerations and velocities resulting from these simple models to what is known experimentally for the actual birds and what previous CFD models have estimated.

Additional Key Words and Phrases: Biomechanics, irrotational potential flow, birds, gannets, diving, water impact

---

## 1. INTRODUCTION

A variety of seabirds including gannets, boobies, tropicbirds, and brown pelicans utilize the highly specialized mechanism of plunge diving for feeding [Shealer 2002]. Of all plunge-diving seabirds, the gannet is considered the most spectacular [Ropert-Coudert et al. 2004]. In plunge diving, a gannet can spot prey from up to 30 m above the water surface [Lee and Reddish 1981]. From that height, these birds pull their wings back and dive into the water. In such a maneuver, the gannet hits the water's surface speeds as high as 24 m/s [Yang et al. 2012]. It is intuitively expected that the transition from such a low to high density fluid ( $\rho_{air} \approx 1.2 \text{ kg/m}^3$ ,  $\rho_{water} \approx 1000 \text{ kg/m}^3$ ) at such a large speed would result in a large impact force to the head and neck of the bird. However, gannets are very rarely injured during these plunges, and in fact will make up to 100 dives in a single trip [Ropert-Coudert et al. 2004].

Understanding how gannets and other seabirds prevent injury during a dive is of great interest for designing shock absorbing systems. Lots of study, for example, has gone into how woodpeckers avoid injury [Gibson 2006]. Woodpeckers can experience decelerations of up to 600 - 1500 *g*. These birds can survive such accelerations in part due to the fact that all birds can move the upper portion of their beak relative to their brain case (i.e. cranial kinesis). However, scaling arguments show that woodpeckers' small size reduces stress on the brain for a given impact, and the short duration of impact (0.5 - 1.0 ms) increases the tolerable acceleration [Gibson 2006]. Whether gannets experience similar inertial forces when impacting the water and if they use similar mechanisms to prevent injury is currently unknown.

More specific to plunge diving, there is a lot of interest in developing hybrid aerial-underwater ve-

---

This work is the final project report for ESM 6984 - Frontiers in Dynamical Systems  
Faculty Sponsor: Dr. Sunny Jung  
Author's address: Office 12 A Randolph Hall (Basement), Virginia Tech  
email: talcat@vt.edu

hicles that can both launch from and dive into water. Those making these biomimetic robots have so far only adapted the morphology and kinematics of these seabirds while they dive. MIT has developed such a vehicle that is able to fold its wings, plunge dive, and then navigate underwater [Fabian et al. 2012]. Similarly, Liang et al. [2013] have developed a prototype ‘bionic’ gannet in order to try and understand the implications of certain kinematic features of a gannet dive.

However, do gannets actually decelerate upon water impact? While there is little information on the speed these bird’s hit the water (besides the maximum of around 24 m/s), it is known that once underwater a gannet will average a speed of descent of around 3 m/s. This would seem to imply a large deceleration occurring early during the dive. However, when accelerometers were attached to gannets to try and measure this deceleration, Ropert-Coudert et al. [2004] were not able to measure any considerable deceleration during water impact. This is despite the fact that a complex computational fluid dynamics model developed by Wang et al. [2013] estimated decelerations of up to 25  $g$  within the first deci-second of impact. The authors of this paper proposed several hypothesis for why this might be. First, the author’s supposed that their 32 Hz sampling frequency was not fast enough to measure any sharp peak in acceleration. This would mean any large decelerations would have to occur within  $\approx 0.03$  seconds to be able to record a single data point. In order to not be counted as noise, several data points over the large deceleration would have to be recorded. This may be reasonable, as the CFD model reports maximum accelerations at 0.0328 seconds (at an impact velocity if 24 m/s). Next, the authors argued that the plunge posture of gannets have extraordinary hydrodynamic features such as streamlining to minimize or even completely eliminate deceleration on impact.

Due to the conflicting results between experiment and modeling, the goal of this paper is to use simple models to develop an intuition of what forces the bird may be experiencing when it hits the water’s surface. While the CFD model is great for complex shapes, it may be hard to understand the results when they are not what is expected. So while Ropert-Coudert et al. [2004] guessed that the plunge posture of the bird is important to eliminate deceleration, the simulation of the posture’s 3D model still experiences large impact forces. However, does the shape experience less impact force than a cone? Was the acceleration significantly smaller or larger than one would expect from that shape from first principles? These questions are hard to answer for such a complex shape. However, if one models the bird as simply a 2D wedge or a cone, with an angle equal to the angle of its beak, we can build an idea of what sort of accelerations should be roughly expected. Comparing when and at what depth the maximum impact force occurs to what gannets actually do may even shed some light on how gannets may avoid large decelerations.

## 2. MODELING

### 2.1 Derivation of Forces and Conservation of Momentum

In general, we can describe any system by Newton’s second law:

$$\sum_i F_i = Ma = M\ddot{y} \quad (1)$$

where each  $F_i$  is an external force acting on the body (with mass  $M$ ), and  $a = \ddot{y}$  is the acceleration on the body. For the case of the diving bird, we assume that the bird is diving vertically into the water, such that all movement is occurring in the  $y$  direction, allowing acceleration to be written as  $\partial^2 y / \partial t^2 = \ddot{y}$ . For a body plunging into the water, forces to be considered include the force due to gravity ( $Mg$ ), steady state drag,  $F_D = \frac{1}{2}\rho C_d \dot{y}^2 S$ , the buoyancy of the body  $F_B = \rho V_{submerged}$ , the capillary force

due to surface tension  $F_c$ , and the impact force  $F_I$ . This results in the equation:

$$M\ddot{y} = Mg - F_I - F_B - F_C - F_D \quad (2)$$

When dealing with the impact force, it is convenient to think of an amount of fluid  $m$ , known as the added mass, that ‘moves’ with the body. This added mass changes with the depth of the body, and additionally depends on the velocity of the body. The impact force can then be defined by:

$$F_I = \frac{D}{Dt} (m\dot{y}) = \frac{\partial}{\partial t} (m\dot{y}) + \dot{y} \cdot \nabla (m\dot{y}) = m\ddot{y} + \frac{\partial m}{\partial y} \dot{y}^2 \quad (3)$$

where  $D/Dt$  is the material derivative, and it is assumed  $\partial m/\partial t = 0$  (this is due to time being an explicit function of depth, making  $y$  our independent variable). Plugging the above into the total force summation yields:

$$(M + m)\ddot{y} = Mg - F_B - F_C - F_D - \frac{\partial m}{\partial y} \dot{y}^2 \quad (4)$$

This can be rewritten as:

$$\frac{D}{Dt} \left( (M + m)\dot{y} \right) = Mg - F_B - F_C - F_D \quad (5)$$

as  $D\dot{y}/Dt = \ddot{y}$  and  $Dm/Dt = \dot{y} * \partial m/\partial y$ .

It can be argued for the case of a gannet diving that gravity, surface tension, and steady state drag do not contribute greatly to the force summation<sup>1</sup>. However, buoyancy is tricky - it is known that these birds contain lots of air trapped in their feathers that help them accelerate quickly back up to the surface of the water and may even help cushion their dive [Yang et al. 2012]. For the purpose of modeling, however, we want to estimate the maximum expected impact force so for now buoyancy will also be ignored. Therefore, we reduce our equation to:

$$\frac{D}{Dt} \left( (M + m)\dot{y} \right) = 0 \quad (7)$$

This can be simply integrated, with the assumption that  $m(t = 0) = 0$ , and that  $\dot{y}(t = 0) = V_o$ , where  $t = 0$  is when the bird’s beak just touches the water’s surface during the dive (the initial time of impact).

$$MV_o = (M + m)\dot{y} \quad \text{or} \quad \dot{y} = \frac{MV_o}{M + m} = \frac{V_o}{1 + m/M} \quad (8)$$

This is simply conservation of momentum of a fluid with added mass. While this final form completely ignores the effects of surface tension, gravity, buoyancy, and steady state drag, it *does* include the unsteady/instantaneous drag due to the virtual mass.

<sup>1</sup>The non-dimension Navier-Stokes equation can be written as:

$$\partial \vec{v} / \partial t + (\vec{v} \cdot \nabla) \vec{v} = -\nabla p + Re^{-1} \nabla^2 \vec{v} - Fr^{-2} \hat{k} \quad (6)$$

where  $p$  is pressure,  $v$  is fluid velocity,  $Re = \rho V_o D / \mu$  is the Reynolds number and  $Fr = V_o / \sqrt{gD}$  is the Froude number. For large values of  $Re$  and  $Fr$  viscous and gravitational effects become negligible. For water ( $\rho = 1000 \text{ kg/m}^3$ ,  $\mu = 10^{-6} \text{ m}^2/\text{s}$ ), and the approximate length of a gannet ( $D = 1 \text{ m}$ ) at an intermediate impact speed ( $V_o = 10 \text{ m/s}$ ), it ends up that  $Re = 10^{10}$  and  $Fr^2 = 10.2$ . These are large enough values that viscous and gravitational effects can be ignored for the plunging gannet.

As the gannet is relatively large, surface tension and curvature forces will also not contribute greatly to the force equation. As our modeling is mostly concerned with shortly after impact, unsteady drag will ultimately dominate over steady state drag, and thus our steady drag can also be neglected.

As one final step, we can find the acceleration of the body at any point in time by taking the derivative of the velocity with respect to time:

$$\ddot{y} = \frac{\partial}{\partial m} \left( \frac{MV_o}{M+m} \right) \frac{\partial m}{\partial y} \frac{\partial y}{\partial t} = -\frac{MV_o}{(M+m)^2} \frac{\partial m}{\partial y} \dot{y} = -\left( \frac{MV_o}{M+m} \right)^2 \frac{1}{MV_o} \frac{\partial m}{\partial y} \dot{y} = -\frac{\dot{y}^3}{MV_o} \frac{\partial m}{\partial y} \quad (9)$$

as  $\partial/t = \partial/\partial m * \partial m/\partial y * \partial y/\partial t$ . From this acceleration term, the force due to the added mass is simply  $M\ddot{y}$ . All of these equations are valid in both 2D and 3D, which will be useful for our wedge and cone model.

### 2.2 Von Karman's 2D Wedge [Abrate 2011]

It is often useful to first consider models in 2D, as they often lead to a great deal of insight into the physical system considered, and are often much easier to analytically consider. Von Karman approached the problem of a 2D wedge impacting the water's surface by estimating the added mass of the falling wedge. If the amount of water moving with the wedge is assumed to be a half disk of radius  $r$ , the added mass is equivalent to:

$$m = \frac{\pi}{2} \rho r^2 \quad (10)$$

where  $\rho$  is the density of the fluid. If we assume our wedge has a half angle of  $\alpha$  (which is  $\pi/2 - \beta$ , the deadrise angle), we can see that there is a relationship between the half-width  $w$  of the wedge and the depth,  $y$ :

$$w = y \tan(\alpha) = \frac{y}{\tan(\beta)} \quad (11)$$

If it is assumed that the radius of our half disk of water is the same as the half-width of the wedge, then the added mass can be given as:

$$m = \frac{\pi}{2} \rho y^2 \tan^2(\alpha) \quad (12)$$

However, looking at Figure 1, one can see that this is a bad assumption for a narrow wedge. Instead we assume that the water will splash up, resulting the the water being higher than the free water surface a small area around our wedge. We account for that by saying the radius of our half disk of water is the same as the half-width of the wedge at some height  $\gamma y$ . This results in:

$$m = \frac{\pi}{2} \rho \gamma^2 y^2 \tan^2(\alpha) \quad (13)$$

This  $\gamma$  has been shown to change with the angle of the cone, and there are many models to relate  $\gamma$  to  $\alpha$ . At the smallest wedge angle of 0 (so a vertical line),  $\gamma = 1$ . This would result in the radius of the half disk of water to be the depth the structure is submerged - which makes intuitive sense. Mei et al. [1999] contains a graph relating wedge angle to  $\gamma$ , which can be used to find the  $\gamma$  for angles relevant to real birds.

From earlier, we can plug this added mass into the acceleration of the body (eqn.9), yielding:

$$\ddot{y} = -\frac{\dot{y}^3}{MV_o} \frac{\partial m}{\partial y} = -\frac{\dot{y}^3}{MV_o} \pi \rho \gamma^2 y \tan^2(\alpha) \quad (14)$$

Noting that it is possible to write  $\dot{y}$  in terms of just the added mass:

$$\dot{y} = \frac{V_o}{1 + m/M} = \frac{V_o}{1 + \frac{\pi}{2M} \rho \gamma^2 y^2 \tan^2(\alpha)} \quad (15)$$

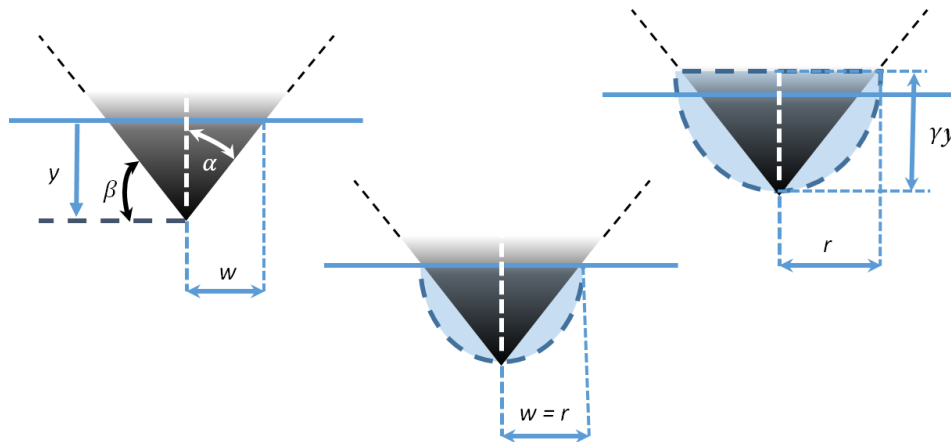


Fig. 1: Diagram of the 2D Wedge Model. Left: defines depth  $y$ , half-width of submerged wedge  $w$ , wedge half angle  $\alpha$  and deadrise angle  $\beta$ . Middle: The half disk of water with radius  $r = w$  which is used to find the virtual mass. Right: Correction for thin wedges and wetting of wedge. The half disk of water is actually has a  $r = w' = \gamma y \tan(\alpha)$ .

the acceleration can be rewritten:

$$\ddot{y} = -\frac{y\dot{y}^3}{MV_o} \pi \rho \gamma^2 \tan(\alpha) = -\frac{y}{MV_o} \left( \frac{V_o}{1 + \frac{\pi}{2M} \rho \gamma^2 y^2 \tan^2(\alpha)} \right)^3 \pi \rho \gamma^2 \tan(\alpha) = -\frac{8yV_o^2 M^2 \pi \rho \gamma^2 \tan^2(\alpha)}{(2M + \pi \rho \gamma^2 y^2 \tan^2(\alpha))^3} \quad (16)$$

The impact force is simply just  $M\ddot{y}$ . The shape of this curve can be seen in Figure 6. It clearly has a maximum at a time very close to the beginning of impact. We can find the depth at which the force will be at its maximum by finding the extrema of the function. This leads to the depth at which we have a maximum force of:

$$y^* = \cot(\alpha) \sqrt{\frac{2M}{5\pi\gamma^2\rho}} \quad (17)$$

In order to be able to plot the force and velocity as a function of time, it is necessary to derive  $y$  as a function of time. Starting with the velocity (eqn.15) and using separation of variables:

$$V_o \partial t = \left( 1 + \frac{\pi}{2M} \rho \gamma^2 y^2 \tan^2(\alpha) \right) \partial y \quad (18)$$

$$t = \left[ y + \frac{\pi}{6M} \rho \gamma^2 y^3 \tan^2 \alpha \right] / V_o \quad (19)$$

as  $\dot{y} = \partial y / \partial t$ .

### 2.3 3D Cone

There has been very little work done on the theoretical slamming of 3D complex objects. This is mostly due to the fact that conformal mapping is very easy in 2D, while extremely limited in higher dimensions [Bergonio 2007]. Therefore, exactly solving for the potential flow of any 3D shape that is not a plate or a sphere must be done computationally (and is really only valid for axisymmetric flows [White 2003]). Therefore, before adequate computational power was available, most analysis was experimental based. Once computational power became available, doing full CFD simulations often proved easier.

There are some analytical results that are quite close to experiment, however. In Shiffman and Spencer [1951], the authors go through the full derivation for the potential flow of a 120 degree angled cone using a ring source. This computation is very difficult, however, and changes non-trivially with different cone angles. Therefore, the authors additionally derived a good approximate theory for calculating the impact force for any cone angle.

Analogous to Van Karman's wedge, it is assumed that an ellipsoid water volume of depth  $y$  and mid-radius  $w$  (the half width of the cone) moves with the cone, and results in the added mass (see Figure 2a). It is possible to assume irrotational, incompressible flow and analytically solve for the velocity and potential flow around this moving ellipsoid. This is a complicated piecewise function that depends on the ratio of  $y$  to  $w$ . In that case one yields:

$$m = k\rho y^3 \tan^3(\alpha) \quad (20)$$

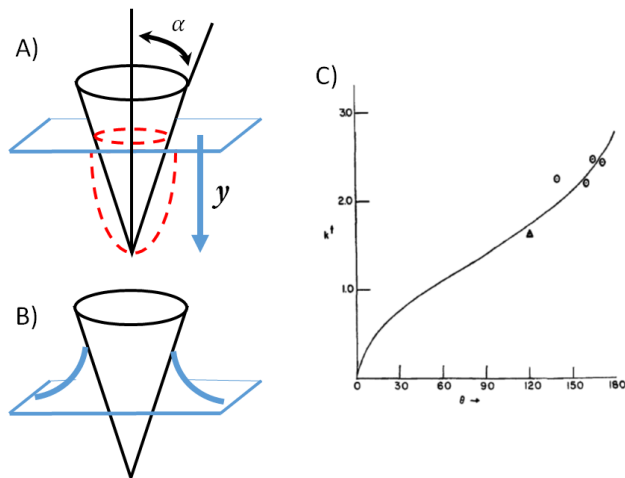


Fig. 2: Shiffman and Spencer [1951]'s 3D cone approximation. A) Cone with half angle  $\alpha$  has an ellipsoid volume (in red) that moves with the cone. This provides information for the added mass. B) Diagram of the wetting correction. Instead of the depth of the cone being purely defined by the resting water surface (the blue plane) the water actually is submerged some extra amount defined by the water that slightly climbs up the cone. C) Plot of corrected  $k$  versus *full* cone angle ( $2\alpha$ ).

where  $\alpha$  is the cone half angle, and  $k$  is a constant that depends on the ratio of  $y$  to  $w$  in a non-trivial manner. An additional correction is made to  $k$  in order to account for splash up of water around the cone (i.e. the wetting of the cone, Figure 2b), which results in a greater effective depth of penetration. The final result is a complicated function relating  $k$  to the cone angle seen in Figure 2c.

While this paper gives an equation for the force estimate, it does not derive it. To do so, just as before, this added mass can be plugged into the conservation of momentum equation derived in section 2.1. Plugging in the cone added mass to (eqn.8) yields:

$$\dot{y} = \frac{V_o}{1 + m/M} = \frac{MV_o}{M + k\rho y^3 \tan^3(\alpha)} \quad (21)$$

Similarly, plugging in the above velocity and the added mass in (eqn.9) results in:

$$\ddot{y} = -\frac{\dot{y}^3}{MV_o} \frac{\partial m}{\partial y} = -\frac{3kM^2\rho V_o^2 y^2 \tan^3(\alpha)}{(M + k\rho y^3 \tan^3(\alpha))^3} \quad (22)$$

By multiplying this acceleration by mass, one returns to the force estimate given by Shiffman and Spencer [1951]:

$$F = \frac{3kM^3\rho V_o^2 y^2 \tan^3(\alpha)}{(M + k\rho y^3 \tan^3(\alpha))^3} = \frac{3mV_o^2}{y(1 + m/M)^3} \quad (23)$$

Of interest, again, is when and where this cone feels its maximum deceleration. By setting  $\partial \ddot{y} / \partial y$  equal to zero, solving for depth yields:

$$y^* = \left(\frac{2M}{7k\rho}\right)^{\frac{1}{3}} \cot(\alpha) \quad (24)$$

Finally, in order to plot the force, velocity, and depth as a function of time, we need to find  $y$  as a function of time. Taking equation (eqn.21) and using separation of variables:

$$V_o \partial t = \left(1 + \frac{k\rho}{M} y^3 \tan^3(\alpha)\right) \partial y \quad (25)$$

$$t = \left[y + \frac{k\rho}{4M} y^4 \tan^3(\alpha)\right] / V_o \quad (26)$$

### 3. IMPLICATIONS FOR THE BIRD

In order to determine the range of velocities, accelerations, and forces these various model's predict the bird goes through, it is necessary to define several parameters. While most of these, such as mass, body length, and velocity are taken from the literature, measurements for the beak half angle and beak length were taken from complete skeleton samples from the Smithsonian Museum in Washington DC. The final parameters used for all simulations can be seen in Table 1. Not included in the table is the density of water, which was taken to be 1000 kg/m<sup>2</sup> for the 2D wedge, and 1000 kg/m<sup>3</sup> for the 3D cone.

Table I. : Simulation values for a diving gannet

Parameter	Value	Source
Mass	3.543 kg	[Wanless and Okill 1994]
Body Length	89 cm	[Wang et al. 2013]
Beak Length	9 cm	See next subsection
Min impact Velocity	3 m/s *	[Ropert-Coudert et al. 2004]
Max impact Velocity	24 m/s	[Ropert-Coudert et al. 2004]
Min beak half-angle	5.5 (deg)	See next subsection
Max beak half-angle	8.0 (deg)	See next subsection

\* This is the average measured speed of descent of the bird once underwater. If the bird does not decelerate when hitting the water, this is theoretically the initial speed.

### 3.1 Wedge half angle estimates from preserved birds

All measurements of beak angle and beak length were made from skull images taken by Sean Gart in 2013 at the Smithsonian Museum in Washington DC. Angles were measured using the angle tool in ImageJ. The beak length was measured in ImageJ as well, and then scaled appropriately using the ruler present in every image. Three species of gannet (Northern gannet, *Morus bassanus*, N = 3; Cape gannet, *Morus capensis*, N = 4; Australasian gannet, *Morus serrator*, N = 2) were analyzed and their results pooled together. Each bird skull had pictures from three orientations: top view, side view, and a head on view, as seen in Figure 3. As most of the bird beaks were bent at the very end, the angle measured from the side view of the skull was very approximate. In addition, the top and bottom of the beak of the birds were not symmetric, resulting in smaller beak angles consistently measured from the side view. The head on view of the skull provided no real information as the cone angle cannot be measured from head on. The results of the measurements can be seen in Table 2 below. For deciding the range of angles to use in simulations, angles measured from the top and side view of the same bird were considered separately.

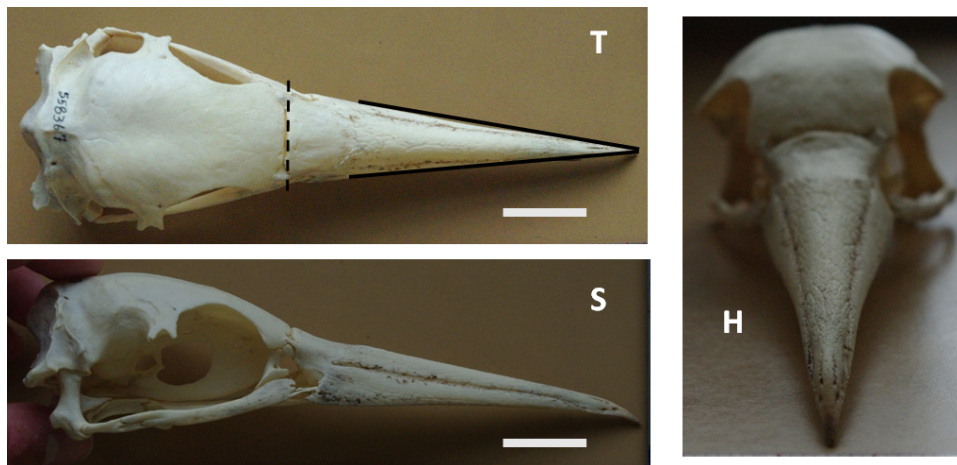


Fig. 3: Representative top (T), side (S), and head on (H) images of a gannet skull used to measure beak length and beak angle. This specimen is *Morus capensis* specimen no. USNM 558376. White bars in the top and side views correspond to 1 inch. The top view shows black lines that are used to measure the beak angle. The beak length is measured from the dotted line to the vertex used for the angle measurement.

### 3.2 Von Karman's 2D Wedge

As the Von Karman wedge estimation yields an explicit function for time as a function of  $y$  (see eqn.19), all simulation values are run for a depth  $y \in [0, 30]$  meters in 0.0001 meter increments, as 30 meters is the deepest depth reported for the Northern Gannet [Brierley and Fernandes 2001; Garthe et al. 2000]. However, note that this approximation is technically only good until a depth of either the beak length (0.09 m), or the body length (0.89 m). This is because this model assumes a wedge that is infinitely long. The real bird, however, has finite length and will completely submerge at some time point. This model cannot tell us anything once the bird is completely submerged. In Figures 4, 5, and 6 one can see the trend of depth, velocity, and acceleration with time. All models were run over 6 velocities (3, 5, 10, 15, 20, 24 m/s) and the two extremes of measured beak half-angles (5.5 deg and 8 deg).  $\gamma$  for both angles were estimated from Mei et al. [1999], with  $(\alpha, \gamma) = (5.5, 1.15)$  and  $(8, 1.2)$ .



Table II. : Bird beak angle and beak length

Species	CAT NUM	View*	Full Cone Angle (deg)	Beak length (m)
<i>Morus bassanus</i>	USNM 16643	T	15.7	0.10
		S	13.4	0.08
<i>Morus bassanus</i>	USNM 347763	T	16.1	0.10
		S	12.3	0.08
<i>Morus bassanus</i>	USNM 502337	T	15.1	0.10
		S	12.4	0.09
<i>Morus capensis</i>	USNM 558370	T	15.8	0.09
		S	11.2	0.09
<i>Morus capensis</i>	USNM 558369	T	15.1	0.10
		S	11.9	0.09
<i>Morus capensis</i>	USNM 558367	T	14.8	0.10
		S	11.6	0.10
<i>Morus capensis</i>	USNM 558368	T	16.0	0.10
		S	11.0	0.09
<i>Morus serrator</i>	USNM 612654	T	14.7	0.09
		S	11.6	0.09
<i>Morus serrator</i>	USNM 620178	T	16.1	0.09
		S	12.0	0.09

\* (T) = top view, (S) = side view

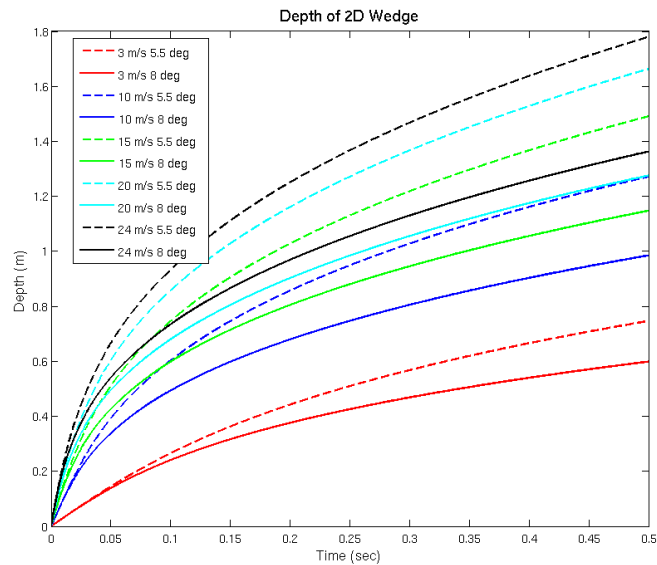


Fig. 4: Depth of the 2D wedge with respect to time. From this graph one can estimate the amount of time that the model is valid under the different parameters. This is the time at which the depth is either the body length (.89 m) or to be more conservative, the beak length (.09 m)

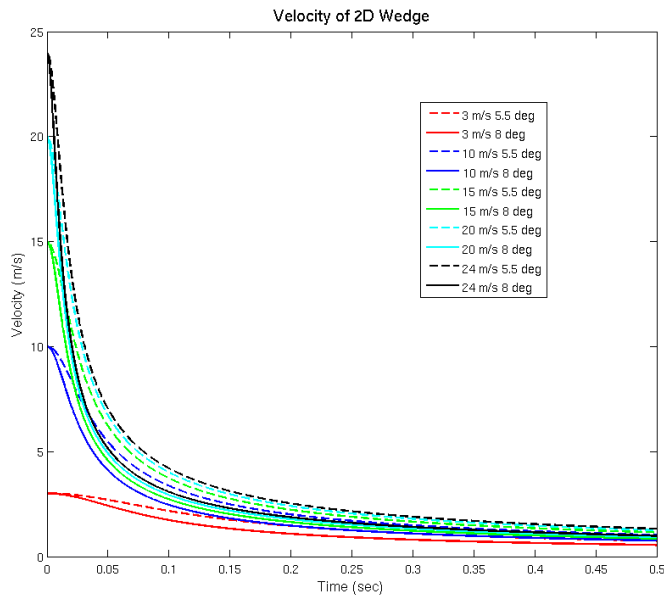


Fig. 5: Velocity of 2D wedge with respect to time. It is interesting to note the asymptote for all angle and initial velocities trending towards 1 - 2 m/s. This is quite close to the underwater descent velocity observed in nature [Ropert-Coudert et al. 2004]

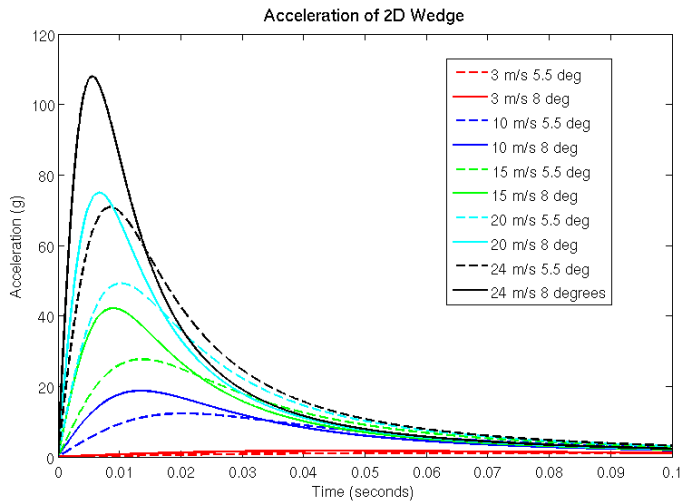


Fig. 6: Acceleration of the 2D wedge with respect to time. This model predicts very high accelerations within the first 10 ms of the dive. For all parameters, this acceleration occurs within the region that the model is still valid (before the bird is completely submerged).

Remember that by taking the derivative of the force, it was found the bird will feel its maximum force at  $y^* = \sqrt{2M/(5\pi\rho\gamma^2)} \cot(\alpha)$  (eqn.17). For a realistic mass, beak angle, etc of the bird this occurs at a depth of about 0.2 meters. In fact, for a given mass of bird, the depth at which the maximum force

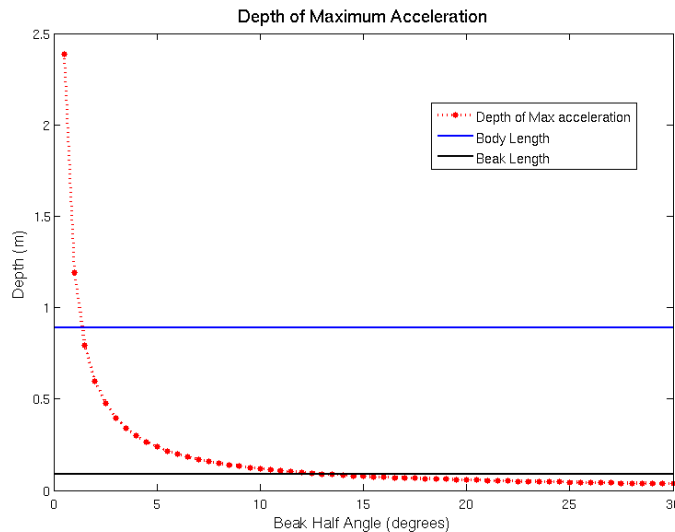


Fig. 7: The depth at which the wedge will reach maximum acceleration as a function of deadrise angle. In blue and black the cutoff depths of body length and beak length are graphed. The argument that maximum acceleration would occur after the bird is fully submerged is only valid for when the depth of maximum acceleration is greater than the cut off values. If the model is no longer valid after the beak length, then physical relevant beak angles result in peak accelerations after the model is no longer valid.

occurs as a function of angle is given in Figure 7. Here,  $\gamma$  for high angles is approximated by the linear equation  $\gamma(\alpha) \approx 1 + .28\alpha$ , which was estimated based on the exact analytical solution given by Mei et al. [1999]. One can clearly see that the bird is completely submerged before this maximum force occurs if their beak half angle is 1 degree or less.

Another key thing to note for this model would be the maximum acceleration the bird would feel due to impacting the water. This occurs again at the depth referred to in (eqn.17). Plugging this value into the equation for acceleration given in (eqn.14) and (eqn.16) yield:

$$\ddot{y}^* = - \left(\frac{5}{6}\right)^3 \gamma V_o^2 \tan(\alpha) \sqrt{\frac{2\pi\rho}{5M}} \tag{27}$$

This means the deceleration is proportional to the square of the initial velocity, just like steady state drag. However, plugging in approximate maximal values ( $V_o = 24$ ,  $\alpha = 10$  degrees,  $\gamma = 1.24$ ) yields deceleration of only  $1372 \text{ m/s}^2$  or  $140 g$ 's. However for realistic beak angle of 11 degrees (half angle  $\alpha = 5.5$  degrees), you get a deceleration of  $695 \text{ m/s}^2$  or  $70 g$ , which for a 2D approximation is at least in the same order of magnitude as Wang et al. [2013]'s CFD model prediction of about  $25 g$ 's.

### 3.3 3D Cone

Similar to the 2D wedge, manipulating the equations in section 2.3 yields an explicit function for time as a function of  $y$ . Therefore, the independent variable of  $y$  was varied between 0 and 30 meters once again. Figures 8, 9, and 10 show the depth, velocity, and acceleration of the cone-bird as a function of time. For both beak angles considered, a  $k$  of 0.2 was estimated from Figure 2c.

From the figures it is immediately clear that this cone model comes extremely close to the full CFD

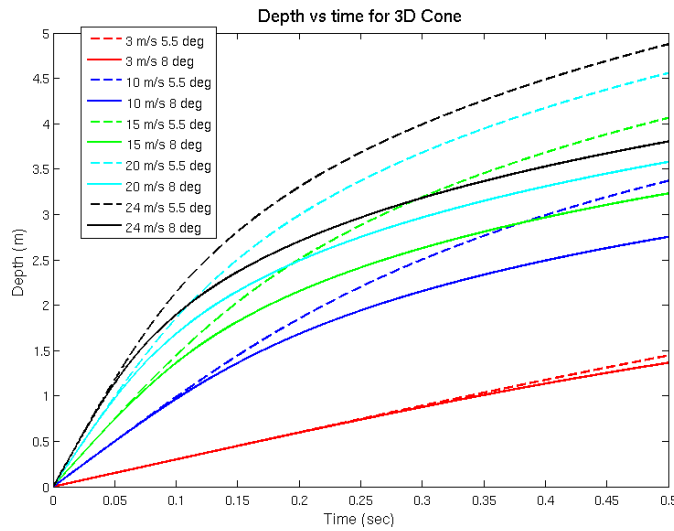


Fig. 8: Depth of the cone with respect to time. From this graph one can estimate the amount of time that the model is valid under the different parameters. This is the time at which the depth is either the body length (.89 m) or to be more conservative, the beak length (.09 m)

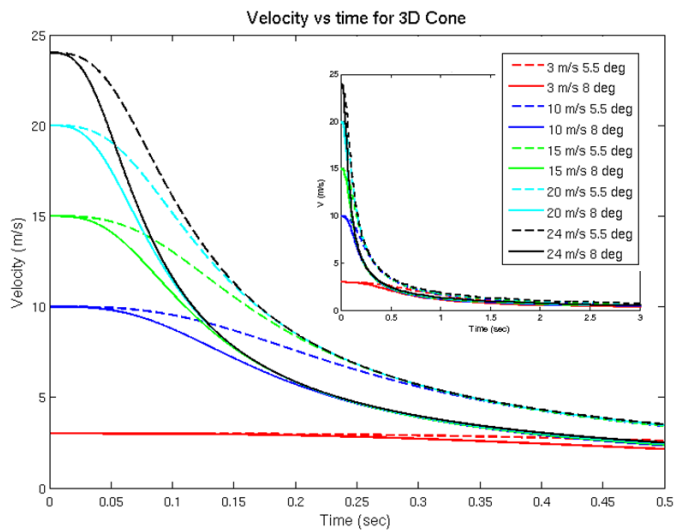


Fig. 9: Velocity of cone with respect to time. It is interesting to note the asymptote for all angle and initial velocities trending towards 1 - 2 m/s. This is especially true when considering the inset, which shows the graph up to diving times seen in nature (about 3 sec long). This is quite close to the underwater descent velocity observed in nature

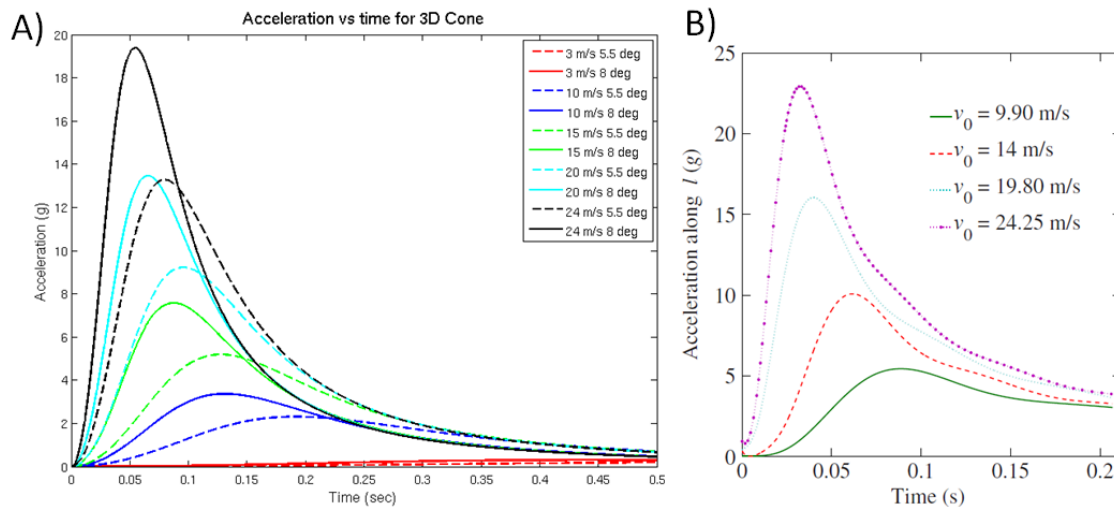


Fig. 10: A) Acceleration of the 3d cone with respect to time. B) Acceleration from [Wang et al. 2013]’s model. Notice that both the timings and the values of maximum acceleration of the cone model are very close to those in the more complicated CFD model.

model [Wang et al. 2013] in both timing of the maximum acceleration and acceleration. This implies that the full 3D posture of the bird does not really mitigate the expected deceleration upon impact. The worst case deceleration using realistic angles and impact velocities is only  $\approx 20g$  endured for about 50 ms. For some insight, humans are alright under accelerations of 80 - 160  $g$  endured over 1 ms, while woodpeckers have measured 600 - 1500  $g$  over 25 ms. So this deceleration is certainly something that other birds could endure without injury quite easily! In terms of whether Ropert-Coudert et al. [2004]’s study could have measured such an acceleration - for even the maximum initial velocity there are large decelerations over a 0.15 second interval at the very least. That would definitely have been picked up by a 32 Hz logger, but only for 3 or so data points (which could be construed as noise). However, there clearly seems to be a trend that the higher the impact velocity, the larger the acceleration and the sharper the acceleration peak. Theoretically, at some higher impact velocity, there might be a large enough acceleration spike over a short enough time that the deceleration would occur within .03 sec, and thus not get picked up by the logger. The probability this is the reason for no measured acceleration *in vivo* however is very low.

Another interesting thing to note is that the velocity (Figure 9) seems to asymptote to around 3 m/s. If the simulation is run until 3 sec, which is the average time gannets are underwater during a dive [Ropert-Coudert et al. 2004], the velocity stays steady at 1 - 2 m/s, which is right in the range of the descent speeds of birds experimentally. This makes sense as the fish these birds are hunting average a speed of around 1 - 2 m/s [Capuska et al. 2011]. If it was known around what depth these birds actually catch fish during a dive, we could compare the time it takes for the bird to reach the 3 m/s range around that depth for different velocities. It may be the case that there is a minimum impact velocity the bird needs to dive at in order to successfully reach the speed underwater necessary to catch fish.

#### 4. CONCLUSIONS AND FUTURE WORK

Overall, modeling a diving gannet as either a 2D wedge or a 3D cone lead to some interesting insights about what accelerations the bird may be expected to encounter. While neither model was able to tease out the reason for contradicting experimental and CFD results for whether the bird feels massive deceleration on water impact (except for providing additional evidence for too low data acquisition rate), we found that the simple cone model (an approximation of the exact potential flow in of itself) was actually extremely close to the CFD model during the early dive (i.e. before the bird completely submerged). This lends credence to the idea that starting with simple models to gain intuition is perfectly valid, and can save a lot of analysis and computation time. It also lends evidence to the fact that the bird's streamlined body is roughly equivalent to a cone, and may allow for future studies to continue to use these simple models.

These simple models yielded the most fruit in adding additional questions to be considered in the future. For example, the long term velocity of the cone was surprisingly close to the swimming velocities of gannet prey. Perhaps there is a link between impact velocity, and reaching the escape velocity of fish within a certain depth of water. Unfortunately, as of yet there is not enough *in vivo* studies with which to compare simulations results.

Future work should definitely work towards adding more forces in these simple models. For example, it is known that gannets and other seabirds trap lots of air in their feathers while underwater. This air allows them to surface quicker due to Boyle's law. These air pockets could theoretically increase the buoyancy force the bird would feel on impact, and therefore perhaps modify the acceleration they feel. In addition, more *in vivo* experiments should be carried out on bird diving. It would be extremely helpful to have real data for velocities immediately before a dive, and maybe even once the bird enters the water. This could be done by filming birds with accelerometers, and then scaling distances to the body length of the bird. With more accurate and detailed live data, it becomes much easier to try and understand the physics behind the phenomenon, especially when real data is compared to simulations and modeling.

#### REFERENCES

- Serge Abrate. 2011. Hull Slamming. *Applied Mechanics Reviews* 64, 6 (2011), 060803.
- Philip Palma Bergonio. 2007. *Schwarz-Christoffel transformations*. Ph.D. Dissertation. uga.
- Andrew S Brierley and Paul G Fernandes. 2001. Diving depths of northern gannets: acoustic observations of *Sula bassana* from an autonomous underwater vehicle. *The Auk* 118, 2 (2001), 529–534.
- Gabriel EMachovsky Capuska, Robin L Vaughn, Bernd Würsig, Gadi Katzir, and David Raubenheimer. 2011. Dive strategies and foraging effort in the Australasian gannet *Morus serrator* revealed by underwater videography. *Marine Ecology Progress Series* 442 (2011), 255–261.
- Andrew Fabian, Yifei Feng, Erika Swartz, Derek Thurmer, and Rui Wang. 2012. Hybrid Aerial Underwater Vehicle (MIT Lincoln Lab). (2012).
- Stefan Garthe, Silvano Benvenuti, and William A Montevecchi. 2000. Pursuit plunging by northern gannets (*Sula bassana*) feeding on capelin (*Mallotus villosus*)". *Proceedings of the Royal Society of London. Series B: Biological Sciences* 267, 1454 (2000), 1717–1722.
- LJ Gibson. 2006. Woodpecker pecking: how woodpeckers avoid brain injury. *Journal of Zoology* 270, 3 (2006), 462–465.
- Davis N Lee and Paul E Reddish. 1981. Plummeting gannets: a paradigm of ecological optics. *Nature* (1981).
- Jianhong Liang, Xingbang Yang, Tianmiao Wang, Guocai Yao, and Wendi Zhao. 2013. Design and Experiment of a Bionic Gannet for Plunge-Diving. *Journal of Bionic Engineering* 10, 3 (2013), 282–291.
- Xiaoming Mei, Yuming Liu, and Dick KP Yue. 1999. On the water impact of general two-dimensional sections. *Applied Ocean Research* 21, 1 (1999), 1–15.
- Frontiers in Dynamical Systems, April 2014.

- Yan Ropert-Coudert, David Grémillet, Peter Ryan, Akiko Kato, Yasuhiko Naito, and Yvon Le Maho. 2004. Between air and water: the plunge dive of the Cape Gannet *Morus capensis*. *Ibis* 146, 2 (2004), 281–290.
- DA Shealer. 2002. Foraging behavior and food of seabirds. *Biology of marine birds* (2002), 137–177.
- M Shiffman and DC Spencer. 1951. The force of impact on a cone striking a water surface (vertical entry). *Communications on pure and applied mathematics* 4, 4 (1951), 379–417.
- TM Wang, XB Yang, JH Liang, GC Yao, and WD Zhao. 2013. CFD based investigation on the impact acceleration when a gannet impacts with water during plunge diving. *Bioinspiration & biomimetics* 8, 3 (2013), 036006.
- Sarah Wanless and JD Okill. 1994. Body measurements and flight performance of adult and juvenile gannets *morus bassanus*. *Ringing & Migration* 15, 2 (1994), 101–103.
- F White. 2003. Fluid Mechanics. 5th ed. (2003).
- Xingbang Yang, Tianmiao Wang, Jianhong Liang, Guocai Yao, Yang Chen, and Qi Shen. 2012. Numerical analysis of biomimetic gannet impacting with water during plunge-diving. In *Robotics and Biomimetics (ROBIO), 2012 IEEE International Conference on*. IEEE, 569–574.